A METHODOLOGY FOR PROBABILISTIC PREDICTION OF FATIGUE CRACK INITIATION TAKING INTO ACCOUNT THE SCALE EFFECT

M. Muniz-Calvente[a], A.M.P de Jesus [b], J.A.F.O. Correia[b], A. Fernández-Canteli[a]

[a]*Dep. of Construction and Manufacturing Engineering. University of Oviedo. Campus de Viesques. 33203 Gijón, Spain*

[b]*INEGI/Faculty of Engineering,University of Porto, Porto, Portugal*

Contact: munizcmiguel@uniovi.es ; telephone:+34 985 18-1967

Abstract

An approach for probabilistic prediction of fatigue crack initiation lifetime of structural details and mechanical components is presented. The methodology applied is an extension of the generalized local model (GLM) to the fatigue case using the fatigue Weibull regression model proposed by Castillo-Canteli. First, the primary failure cumulative distribution function (PFCDF) of the generalized failure parameter is derived from experimental results for a given reference size, taking into account the non-uniform distribution of the generalized parameter (GP) the specimens are submitted to. The adequacy of the GP is presumed, ensuring uniqueness of the derived PFCDF as a material property, irrespective of the specimen shape and size, and the test chosen to this end. Next, the GP distribution is obtained by a finite element calculation and the PFCDF is applied to each finite element, considering the scale effect, to derive the probability of failure for the whole component. The suitability of the proposed approach is illustrated twice: first, assessing simulated data in a theoretical example, and second, evaluating experimental fatigue life results for riveted joints from the historical Fão Bridge. The PFCDF for the puddle iron from the bridge is calculated from standard tensile specimens, from which the initiation fatigue lifetime of the riveted connections is predicted and compared with the experimental results. In this way, the transferability from standard tests to real components is demonstrated.

Keywords: Generalized Local Model, Primary failure CDF, Probabilistic fatigue, Scale effect, Weibull distribution.

Nomenclature

B: Threshold number of cycles of the Castillo-Canteli model

C: Fatigue limit of the Castillo-Canteli model

CDF: Cumulative distribution function

EFCDF: Experimental failure cumulative distribution function

GLM: Generalized local model

GP: Generalized parameter

N: Number of cycles

N_{ini}: Lifetime to crack initiation

PFCDF: Primary failure cumulative distribution function

P_{fail}:Probability of failure

P_{int}: Integrated probability of failure

S: Stress

S_{ref}: Reference size

SWT: Smith-Watson-Topper parameter

V: Normalized variable of the Castillo-Canteli model)

λ: Weibull location parameter

β: Weibull shape parameter

δ: Weibull size parameter

ε: Strain

1. Introduction

Probabilistic fatigue models are indispensable to take into account the different sources of uncertainty inherent to fatigue lifetime analysis, which become apparent as scatter of the experimental data. Contrary to deterministic models, probabilistic ones provide the solution to extrapolate fatigue data from simple uniaxial tension or bending tests to predict lifetime of components or even large engineering structures, such as bridges, ensuring transferability, in which the scale and shape effect are important issues to be considered. It is worth mentioning that, besides probabilistic models, there are also deterministic models based on fractal theories that allow the scale effect to be taken in a natural way [1-3].

During the last decades, different probabilistic fatigue models have been proposed in the literature to derive probabilistic S-N fields. Already in 1972, Bastenaire [4] proposed a method for the statistical evaluation of constant stress amplitude fatigue test results. After that, different models and improvements have been developed, such as the study of cumulative damage developed by Bogdanoff (1985) [5] based on the so-called B-model, or the inclusion of censored life data proposed by Escobar and Meeker (1999) [6]. Furthermore, other relevant examples of probabilistic fatigue models are presented by the works of Pascual and Meeker [7], Spindel and Haibach [8], and Schijve [9]. The Weibull fatigue approach proposed by Bolotin [10,11], denoted “half phenomenological” by the author, is derived from scalar damage measures, and deserve special recognition since it anticipates the Weibull regression model for the S-N and ε-N fields as proposed by Castillo and Canteli [12]. The latter merges as the solution of a functional equation, resulting from the necessary compatibility condition to be accomplished along the whole S-N field between both distributions, that of lifetime for given stress (or strain) range and that for stress (or strain) range for given lifetime. An interesting point is that the Bolotin model fulfils the above mentioned compatibility condition, without being contemplated as an initial requirement of the model by the author [10,11].

Subsequently, Correia *et al.* [13] have extended this model to more general damage criteria, by considering the Smith-Watson-Topper (SWT) parameter as a reference for the fatigue damage, thus leading to the probabilistic SWT versus number of cycles field (p-SWT-N). An extension to more general parameters of energetic character is justified in reference [14].

Usually, the p-S-N field (probabilistic stress versus number of cycles field), resulting from probabilistic Weibull fatigue models, is applied without considering the influence of the reference parameter distribution due to the geometry and size of the specimens tested and loading conditions. This even hinders a comparison between different testing programs. Occasionally, the length effect on the fatigue lifetime of long elements has been explicitly investigated [15], but generally the influence of the varying distribution of the reference parameter over the specimen (usually referred to stress or strain) is neglected, leading to an erroneous cumulative distribution function (CDF) of failure or mistaking the reference specimen size. This limitation in previous models impedes a correct transference of the fatigue characterization resulting from small-scale specimens tested in the laboratory to the practical design, so that the prediction of the fatigue crack initiation life of real components and structures will be unreliable.

To proceed to the fatigue lifetime forecasting of real components, the so-called primary failure cumulative distribution function (PFCDF) must be derived by applying the "generalized local model" (GLM), developed in previous works of the authors for quasi-static failure predictions [16-18]. The PFCDF characterizes the material failure in a probabilistic way representing the probability of failure for a given reference size of the material as a function of the generalized parameter, this being uniformly distributed over that size. The PFCDF could be derived from any specimen geometry and size even in the case of non-uniform distribution of the selected reference parameter along the specimen, so that any type of test may be adopted to characterize the material. In this way, the assessment of the probabilistic failure of a real component for any geometry, size and loading conditions is possible.

The GLM, initially developed to predict the quasi-static failure of components made of brittle materials such as structural members of glass, may be extended to fatigue lifetime prediction based on the normalizing property of the Weibull fatigue model proposed by Castillo-Canteli [12], assuming validity of the weakest link principle. In particular, a probabilistic prediction of the fatigue crack initiation of structural details or mechanical components of engineering structures is feasible, taking into consideration the specimen shape and size, and the distribution of the critical fatigue damage parameter. The combination of both models (GLM and Weibull fatigue model) ensures the uniqueness of the PFCDF, which can be derived irrespective of the test selected to this aim. As a consequence, assuming adequacy of the fatigue damage parameter adopted, the probabilistic methodology proposed in this paper guarantees the transferability of the fatigue test results from laboratory specimens to components in a natural way adding shape and scale effect analysis, which is the main contribution of this paper.

This paper is organized as follows: first, a brief review of the above two models constituting the basis of the combined methodology presented, i.e. the GLM and the Weibull model of Castillo-Canteli, is exposed. Subsequently, the description of the iterative process for deriving the PFCDF is illustrated by a theoretical example, using simulated fatigue test data. Finally, a practical example, based on experimental results from fatigue tests conducted on material extracted from references [13,14], is presented to demonstrate the applicability of the proposed methodology.

2. Overview of the Weibull probabilistic fatigue model

The Weibull probabilistic regression model, proposed by Castillo-Canteli [12], defines the S-N or ε-N fields as hyperbolic shaped percentiles, i.e. by hyperbolic curves representing the same probability of failure (see Fig. 1a).

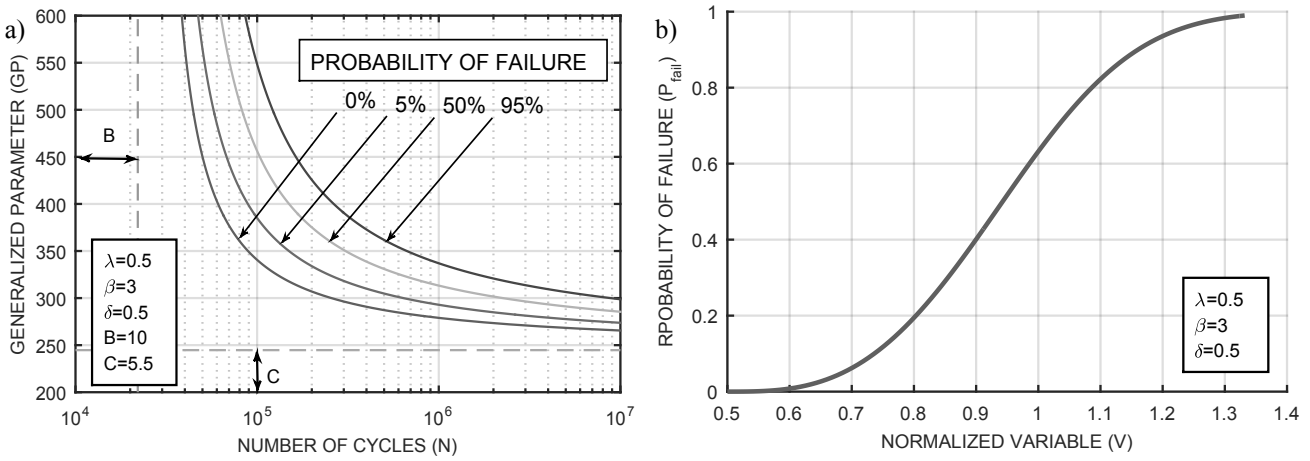

Figure 1. Illustration of the probabilistic fatigue field resulting from the Weibull model [12]: a) Probabilistic Generalized parameter versus Number of Cycles field (p-GP-N) and b) CDF of the normalized variable V.

This model can be extended to any kind of generalized fatigue parameters, as is the case of energetic ones, resulting from possible combinations of stresses and strains to define a particular fatigue failure criterion [9]. In this way, the relationship among a generalized parameter (GP) related to the crack initiation, the lifetime to crack initiation (N_{ini}), and the probability of failure (P_{fail}) may be expressed as:

$$P_{fail} = 1 - exp\left[-\left(\frac{V-\lambda}{\delta_{ref}}\right)^{\beta}\right] \qquad (1)$$

where:

$$V = (log\ GP - C)(log\ N_{ini} - B) \qquad (2)$$

and λ, β and δ_{ref} are the location, shape and scale parameters, respectively, of the Weibull distribution, *V* the normalized variable allowing the GP-N field (i.e. S-N or ε-N) to be reduced to a simple CDF, and B and C the two asymptotes of the Castillo-Canteli model defining the threshold value of lifetime and the fatigue limit, respectively. The location parameter, λ, represents the smallest value of V at which failure may occur. It should be noted that the Weibull cumulative distribution function of the normalized parameter, *V*, represents the probability of failure, P_{fail} for a specifically selected reference size, S_{ref}, to which the scale factor δ_{ref} is related (see Fig. 1b). Both the scale, δ_{ref}, and shape, β, parameters, are associated with the scatter of the experimental results, being the first one related to the specimen size S_{ref} and the second one to the fracture mechanism. The conversion of that CDF to another specimen size, S_{new}, only requires the consideration of a new scale parameter defined as:

$$\delta_{new} = \delta_{ref}\left(\frac{S_{ref}}{S_{new}}\right)^{1/\beta} \quad (3)$$

Accordingly, the relationship between *V* and the probability of failure for the new size, S_{new}, becomes:

$$P_{fail,S_{new}} = 1 - exp\left[-\frac{S_{new}}{S_{ref}}\left(\frac{V-\lambda}{\delta_{ref}}\right)^{\beta}\right] \quad (4)$$

Figure 2a illustrates the influence of a change of the scale parameter on the CDF of the normalized variable, *V,* evidencing that the scatter varies inversely with the specimen size. As a practical consequence, the model states that under the same load conditions, the S-N fatigue field for larger specimens exhibits less scatter than for smaller specimens. Figure 2b shows the 5%, 50% and 95% isoprobability failure curves for three different scale parameter values.

The scatter and the expected number of cycles to failure are lower for larger sizes ($\delta_{ref} = 0.5$) than for medium ($\delta_{ref} = 1.0$) and shorter specimens ($\delta_{ref} = 1.5$).

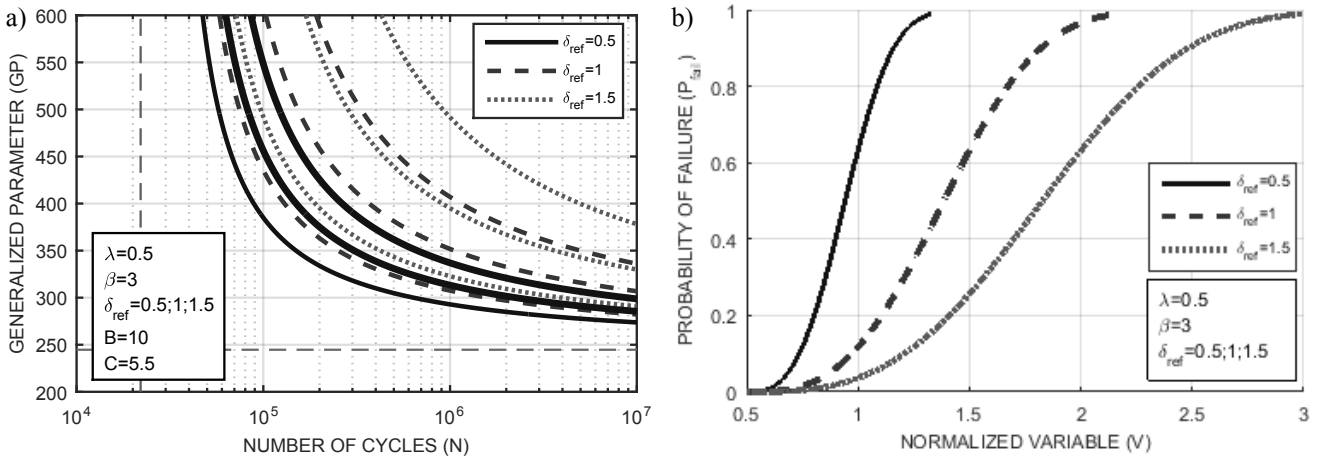

Figure 2. Influence of the scale parameter on the probabilistic fatigue fields: a) Probabilistic fields of the generalized parameter versus number of cycles (p-GP-N); b) corresponding CDFs of the normalized variable (V).

The Weibull regression model [12], as given in Equation (4), includes the scale effect allowing the experimental results for a testing program comprising different specimen sizes to be evaluated, providing a unique representative cumulative distribution function related to a chosen reference size. This model can be applied straightforwardly to cases where the generalized parameter shows a uniform distribution all over the specimen or component, as is the case of uniaxial tensile tests where the specimen section can be assumed constant. In such cases, the reference size, S_{ref}, can be defined, alternatively, as the length, area or volume subjected to this uniform distribution of the GP.

However, fatigue tests are generally performed on specimens with varying cross-section or real prototypes and components, which most likely exhibit a non-uniform distribution of the reference parameter under the testing loads. Under these conditions, the use of the Castillo-

Canteli model [12], according to its traditional definition, could be incorrect because it is based on the unique local maximum value of the reference fatigue parameter (usually stress or strain ranges) what implies neglecting its distribution along the specimen and, as a consequence, the possible scale effect. For this reason, a previous determination of the reference size (S_{ref}) based on the generalized local model [16-18] applied to the particular test specimen geometry is required to determine the real primary failure cumulative distribution function (PFCDF), and proceed subsequently to the fatigue life prediction of components.

3. Description of the proposed methodology

3.1 Introduction to the generalized local model

The generalized local model (GLM) [16-18] consists in an iterative procedure allowing the PFCDF to be obtained for a chosen generalized parameter (GP) and a specific reference size. The PFCDF, as already mentioned, represents the probability of failure for a given value of the generalized parameter, this being uniformly distributed over the reference size. Along the iterative process, the experimental failure cumulative distribution function (EFCDF) is transformed to the PFCDF, taking into account the specimen geometry and size, or even test modality, irrespective of the possible varying distribution exhibited by the selected generalized parameter (GP) during the test. In this way, the PFCDF, as related to a uniform GP distribution and reference size, represents a material failure property ensuring transferability of the fatigue properties from any specimen shape and size, and test type thus allowing a reliable probabilistic failure assessment of a real component for any geometry and loading conditions to be achieved.

3.2 Description of the iterative process

In the following, the iterative process applied to derive the PFCDF (Fig. 3), is illustrated by an example using simulated fatigue test data relative to the failure of uniaxial tensile test with variable section specimen, as depicted in Fig. 4. It implies the combination of the GLM and the Weibull regression model proposed by Castillo-Canteli [12].

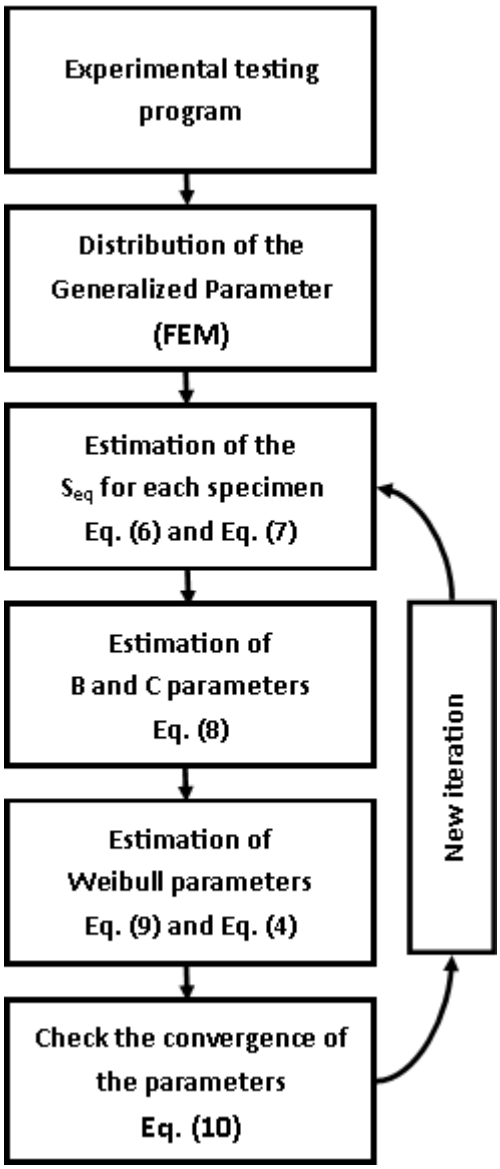

Figure 3. Iterative procedure for estimation of the five parameters of the *PFCDF*.

The distribution of the axial stress along the specimen, this time taken as the generalized parameter to which failure is referred, is given as a function of the cross-sectional area (A) and the applied load (P):

$$GP = \frac{P}{A} \qquad (5)$$

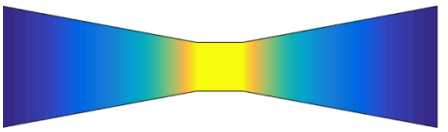

Figure 4. Schematic GP distribution along the specimen surface.

To simulate experimental results, a set of model parameters is assumed, namely: λ=0.5, β=3, δ_{ref}=0.5, C=5.5, B=10, which implies the definition of the primary failure cumulative distribution function (PFCDF) (see Eq. 4). Next, an experimental program comprising forty test results is simulated by selecting twenty different GP ranges and generating two random fatigue lives. To this end, two random values in the interval 0-1 are drawn for each GP range, which are introduced as ordinate values into the PFCDF providing the prospective fatigue lives as illustrated in Fig. 5a. columns 1, 3 and 4 in Table 1 show the simulated test results obtained. A comparison between the S-N field resulting from the assumed PFCDF and the simulated test results is shown in Fig. 5b.

Once the simulated data are generated, the values of lifetime and load ranges reported in Table 1 are used to derive the theoretical PFCDF by applying the new methodology presented in this paper, and compare it with the PFCDF resulting for the parameters used to generate the simulated data.

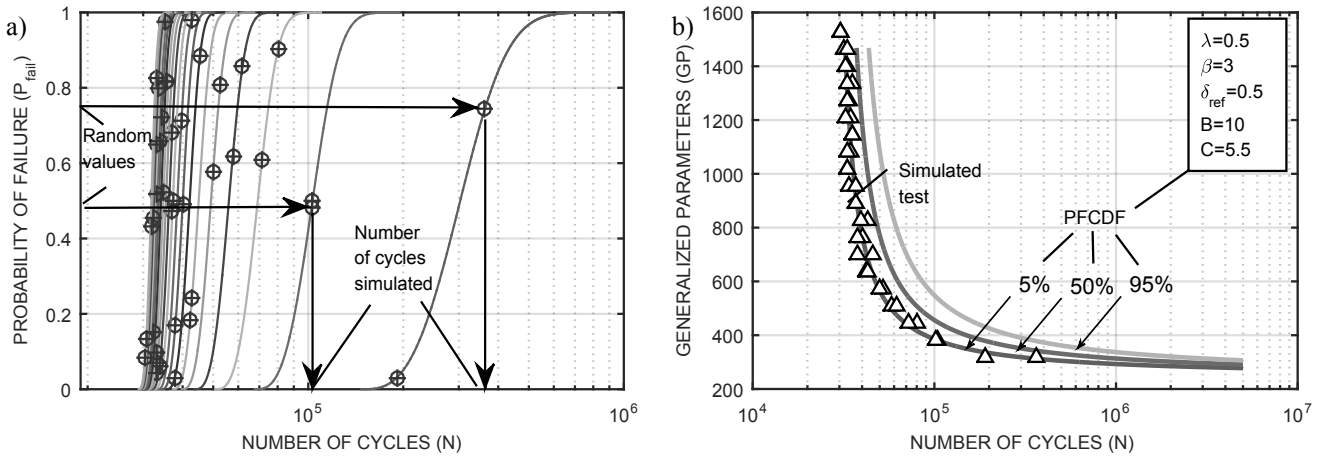

Figure 5. a) Representation of the simulation process; b) Comparison between the S-N field resulting from the assumed PFCDF and the tests results from the simulation.

P (Max. Load)	Max. Value of GP (Critical Parameter)	N1 (cycles)	N2 (cycles)
100000	318.31	190586	362936
120000	381.97	103199	102376
140000	445.63	80466	71472
160000	509.30	57659	61991
180000	572.96	52682	49957
200000	636.62	42248	42814
220000	700.28	45435	37707
240000	763.94	39992	37912
260000	827.61	42789	39663
280000	891.27	37254	37115
300000	954.93	33786	37080
320000	1018.59	32932	33253
340000	1082.25	34820	32901
360000	1145.92	35441	35437
380000	1209.58	34428	32298
400000	1273.24	33710	33243
420000	1336.90	35132	33255
440000	1400.56	33422	32298
460000	1464.23	31925	33172
480000	1527.89	30413	30670

Table 1. Simulated tests based on Monte Carlo sampling technique.

In the following, each step applied for the derivation of the PFCDF in the case of fatigue crack initiation is described.

STEP 1: Experimental testing program

First, the proposed methodology requires carrying out a set of fatigue failure tests in the laboratory recording the load ranges applied and the corresponding number of cycles until failure. In this example, as mentioned above, 40 tests were simulated as initial values to start the iterative process (see Table 1).

STEP 2: Distribution of the critical parameter

The load data resulting from the previous step are used to determine the local distribution of the generalized parameter all over each specimen. An analytical expression of the GP distribution, as presumed in a former work [19], is not required since the GLM methodology allows the GP distribution to be found numerically (e.g. by means of FEM), and to be subsequently used for the calculation of the failure probability [20]. In the present case, the GP distribution, identified with local axial stresses, is obtained using Eq. (5).

STEP 3: Estimation of the equivalent size for a test failure

The equivalent size, $S_{eq,i}$, is defined as the size that subjected uniformly to the maximum value of the GP occurring at the test failure, provides the same probability of failure than that arising by the real specimen subjected to the actual varying distribution of the GP at failure. It may be found as:

$$S_{eq,i} = -\log\left(1 - P_{int,i}\right) S_{ref}\left[\frac{\delta_{ref}}{V_i - \lambda}\right]^{\beta} \quad (6)$$

where $P_{int,i}$ is the integrated probability for the *i*-specimen at failure, which results as the combination of the probabilities of failure, denoted $P_{fail,\ \Delta S_{ij}}$, for all the elements being part of the specimen according to the relation:

$$P_{int,i} = 1 - \prod\left(1 - P_{fail,\ \Delta S_{ij}}\right) = 1 - \prod\left(exp\left[-\frac{\Delta S_{ij}}{S_{ref}}\left(\frac{V_{ij} - \lambda}{\delta}\right)^{\beta}\right]\right) \quad (7)$$

where ΔS_{ij} and V_{ij} are the size and the normalized variable, respectively, the latter being dependent on the generalized parameter, GP_{ij}, for the *j*-element of the *i*-specimen.

Obviously, the value of $S_{eq,i}$ cannot be estimated from Eq. (6) and (7) in the first iteration, because it depends both on the values of *B*, *C* and on the three Weibull parameters, which are still unknown for the time being. For that reason, $S_{eq,i}$ should be randomly assigned in the first iteration. In order to reduce the number of iterations, an initial estimate of $S_{eq,i}$ close to 80% of the real specimen size can be adopted to start the iteration process.

STEP 4: Estimation of the parameters B and C

Although all tested specimens exhibit the same size and geometry, the varying GP distributions are specific for any of the load values at failure. Accordingly, the transformation of those varying GP distributions at failure into the corresponding equivalent uniform GP distributions for the different specimens implies a particular equivalent size for each specimen tested. For this reason, *B* and C must be determined by minimizing the least square equation proposed in reference [12] with respect to *B*, *C* and μ_1, μ_2, … μ_t for different sizes:

$$Q = \sum_{i=1}^{n}\left(log\ N_i - B - \frac{\mu_i}{log\ GP_i - C}\right)^2 \quad (8)$$

where μ is the median value for each of the different specimen sizes, *n* is the sample size and GP_i and N_i are the maximum value of the critical parameter and the number of cycles to failure for the i-th specimen, respectively.

The main problem in the minimization process of this function lays in the fact that the number of equivalent sizes obtained equals the number of specimens tested. This means that, in the case of *N* tests, the number of the parameters to be optimized in Eq. (8), taking into account *B* and *C*, is *N*+2, so that a good estimate of *B* and *C* cannot be achieved using this method.

To solve this problem, similar equivalent sizes are grouped at staggered intervals, as shown in Fig. 6. In this way, the number of μ_t variables implied in the problem is lowered thus expediting the convergence of the model.

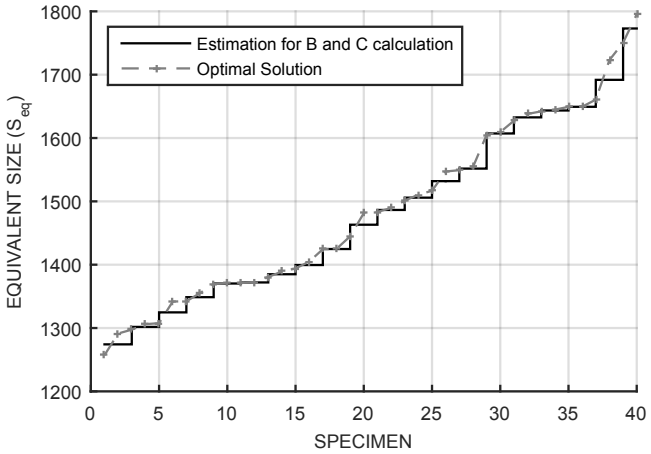

Figure 6. Sorted equivalent sizes.

STEP 5: Estimation of the Weibull parameters

Once *B* and *C* are determined, it is possible to calculate the dimensionless variable V_i and the integrated probability P_{int} for each specimen using Eqs. (2) and (7), respectively. Thereafter, the test results are sorted in ascending order, and the corresponding values of P_{int} are assigned to them.

Finally, the probability of failure for each of the specimens can be obtained using a plotting point position rule, as the Bernard's one given by:

$$P_{fail} = \frac{i - 0.3}{N + 0.4} \qquad (9)$$

After having determined the probability of failure P_{fail}, the equivalent size $S_{eq,i}$ and the maximum value of V_i for each specimen, the values of λ, β and δ are fitted using Eq. (4) [21].

STEP 6: Quality degree of the solution obtained

The five parameters of the Weibull regression model define the PFCDF of the material, which allows the failure probability for any type of component and load to be determined. Thus, the PFCDF can be applied to compute the probability of failure of the experimental results performed. Obviously, the resulting PFCDF from the first iteration does not provide a good estimation of *p-GP-N* or *V-p* curves, because the calculated values of the equivalent sizes are not still accurate.

However, after some iterations, the values of the parameters B, C, λ, β and δ remain practically constant from one iteration to the next one. Thus, the resulting *p-GP-N* and *V-p* curves could be considered the final solution (see Fig. 7).

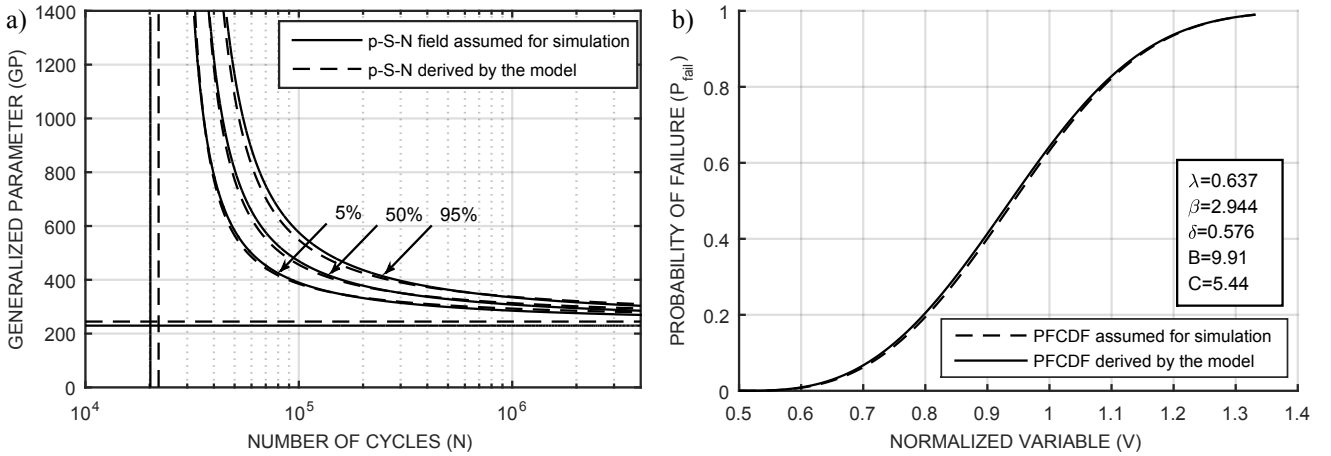

Figure 7. Comparison between the PCDFF assumed and that obtained from simulated experimental results.

As can be seen at Fig.7, the methodology proposed provides a good estimation for the PFCDF related with the normalized variable V but also for the probabilistic lifetime field. The coincidence between the assumed and fitted PFCDF and p-GP-N percentiles demonstrates that the model is useful to derive the fatigue PFCDF as a material characteristic, taking into account the local values of the GP at failure conditions, thus permitting the consideration of the size effect in the evaluation of experimental results.

The fitting process is fulfilled when the absolute variation of the sum of all the parameters intervening in the definition of the GP-N field, i.e. the Weibull parameters and B and C as asymptotic parameters, becomes less than a prescribed small threshold value, ε :

$$|\lambda_i - \lambda_{i-1}| + |\beta_i - \beta_{i-1}| + |\delta_i - \delta_{i-1}| + |B_i - B_{i-1}| + |C_i - C_{i-1}| < \varepsilon \qquad (10)$$

Otherwise, the iterative process continues returning to step 3.

4. Example of application

This section illustrates the practical application of the proposed methodology. It consists in the probabilistic prediction of the fatigue crack initiation lifetimes for real riveted joints based on the PFCDF obtained from fatigue tests performed in the laboratory using standard dog-bone specimens made of the original material from the bridge. For the derivation of the PFCDF the non-uniform stress and strain distributions at the riveted joints are taken into account.

The material (puddle iron) was extracted from the Fão road bridge [22,23], built at the end of 19th century to cross the Cávado River at Esposende, in the northwest region of Portugal, upon the design of Abel Maria Mota (Fig. 8).

4.1. Material properties

Some original side diagonals of the bridge were replaced by new ones during the rehabilitation of the Fão bridge some years ago, allowing the extraction of original material (puddle iron) to be used in the experimental program. Tables 2 and 3 summarize, respectively, the main mechanical properties and the chemical composition of the material, evaluated by spark emission spectrometry technique [22].

Figure 8. The Fão riveted metallic bridge [22].

Young Modulus (GPa)	Yield Strength (MPa)	Ultimate tensile Strength (MPa)	Elongation at fracture (%)	Reduction in cross section (%)
198.7	220	359	23	13

Table 2. Tensile properties of the material from Fão bridge

C	Mn	Si	P	S
0.09	0.13	0.06	0.14	0.007

Table 3. Chemical composition of the material, puddle iron (% weight)

4.2. Experimental results and calculation of the PFCDF

Two different experimental programs were performed: a) 35 uniaxial tension/compression tests were carried out under strain control using dog-bone specimens (see Fig.9), according to the ASTM E606 standard [24], and b) 15 riveted joint tests (see Fig.10).

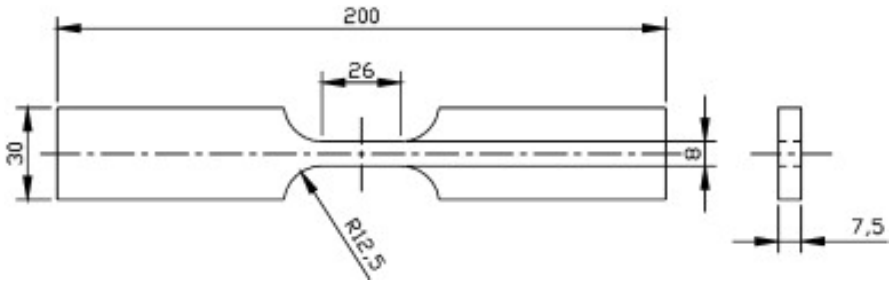

Figure 9. Uniaxial smooth dog-bone specimen: technical representation (dimensions in mm).

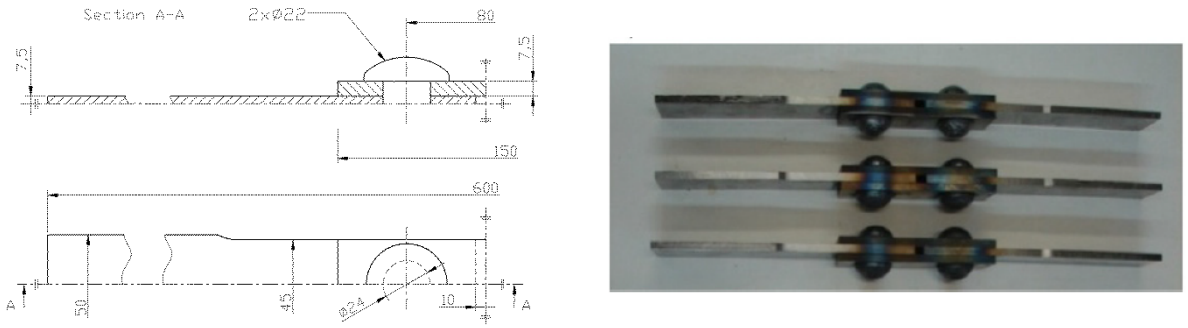

Figure 10. Double shear riveted joints: (left) technical representation (dimensions in mm) and (right) photograph of some riveted joints [25,26].

Though two different strain ratios (R_ε=0 and R_ε=−1) are considered in the first experimental program, all results are fitted to a unique PFCDF following the procedure described above after

verifying that the influence of that parameter on the final fatigue life results become negligible [15]. The reference size is related to the central surface area of the specimen, while the generalized parameter is identified with the uniaxial strain range measured during the fatigue tests according to the experience of previous works using this material [25,26]:

$$S_{ref} = 806\ mm^2 \qquad GP = \Delta\varepsilon_a\ [\mu\text{strain}] \qquad (11)$$

Although the experimental results from this practical application are disseminated in the literature as total fatigue lifetimes, and the methodology proposed in the paper is only applicable to fatigue crack initiation, different numerical analyses performed by FEM [27] prove that the total fatigue life of these specimens is mainly determined by the crack initiation phase, so that the propagation phase may be neglected. The application of the methodology described in the previous section to the puddle iron from the Fão bridge leads to the following model parameters: B = 0, C=3.57, λ=12.82, β=7.12 and δ=11.53. The resulting fatigue GP field, i.e. the iso-probability or percentile curves, and the PFCDF are shown in Fig. 11.

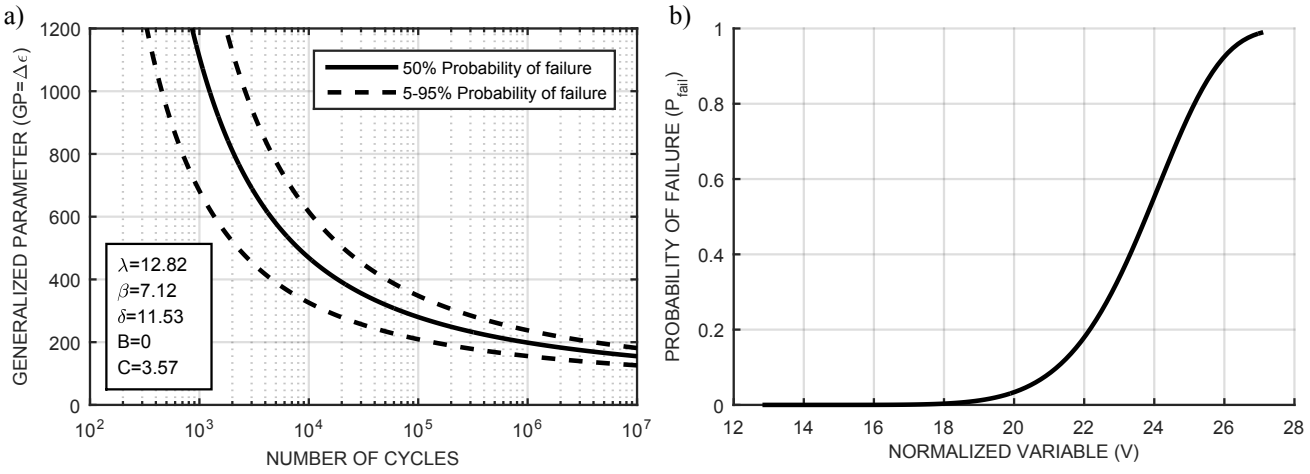

Figure 11. PFCDF for the Puddle Iron of the Fão Bridge obtained by smooth specimens subjected to uniaxial load.

4.3. Prediction of failure for the riveted joints

The PFCDF obtained is used to derive the probabilistic fatigue crack initiation fields for the riveted joint shown in Fig. 10. To compute the local elastoplastic strains in the riveted connection, a three-dimensional FE model is applied using the ANSYS® commercial code [27] (Fig. 12). Taking advantage of the existing symmetry, only 1/8 of the geometry is modelled. Additionally, a convergence study is performed to minimize the mesh influence on results, whereby that represented in the Fig. 12 is the final one adopted in the FE analysis. According to the solution already studied by the authors for this riveted joint [13], a friction coefficient of 0.3 is assumed between the specimen plates of the rivet connection and a low clamping stress (25MPa) is supposed to be provided by the rivet. More details about the mesh, contact model and rivet clamping effects application can be found in reference [26]. With the aim of obtaining the probabilistic fatigue crack initiation field, 15 different nominal tensile stresses are applied in the simulation: $\Delta\sigma_j$={50 60 70 80 90 100 110 120 130 140 150 160 170 180 190 200}MPa.

As recommended in reference [28], the Twice Yield Method (TWM) is applied to extract the local elastoplastic strain ranges at each load level as a more efficient procedure, from a numerical point of view, than a cycle-by-cycle elastoplastic analysis.

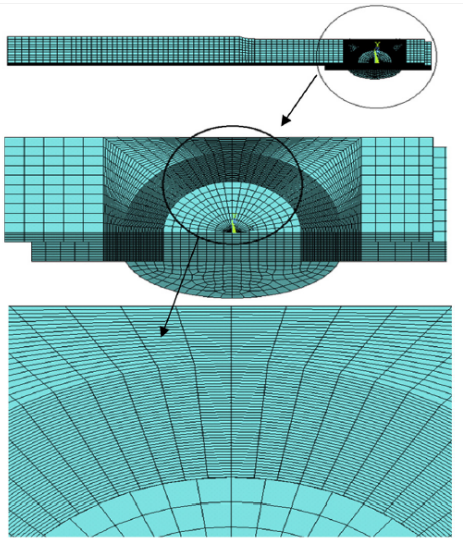

Figure 12. Finite element mesh of the 1/8 of the riveted joint [26].

After computing the elastoplastic strain range field, the number of cycles related to a certain global probability of failure for each load level is obtained with the equation:

$$P_{fail,j} = 1 - \prod_{i=1}^{n} \left(exp\left[-\frac{\Delta S_i}{S_{ref}} \left(\frac{(log\,\Delta\varepsilon_{ij} - C)(log\,N - B) - \lambda}{\delta} \right)^{\beta} \right] \right) \quad (12)$$

where B, C, λ, β, δ and S_{ref} are the Weibull parameters as fitted above, $\Delta\varepsilon_{ij}$ is the local elastoplastic strain range of the finite element i related to the nominal stress range $\Delta\sigma_j$, ΔS_i is the size of the element i, and $P_{fail,j}$ is the selected global probability of failure for the specimen j. Figure 13 depicts the prediction of the *p-S-N* field for the riveted joint. The good agreement between the predicted failure probabilities of the rivet joint resulting from Eq. (12) and the experimental results tested in the laboratory demonstrates the satisfactory applicability of the model from a simple PFCDF to a case with a complex distribution of the critical parameter.

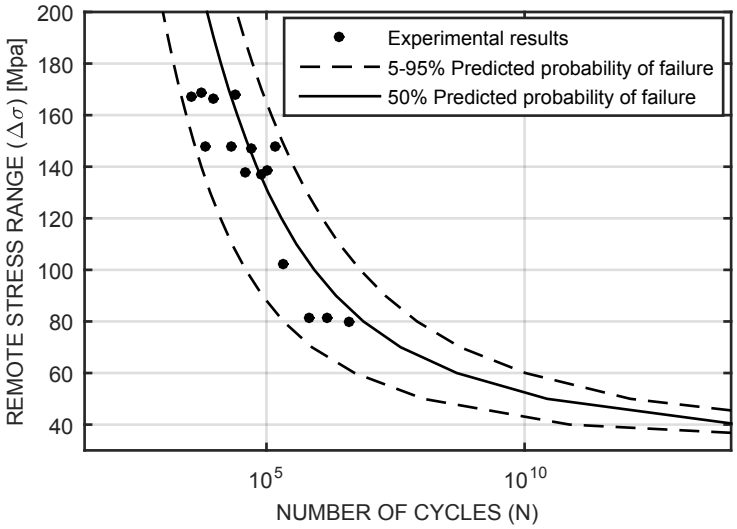

Figure 13. Comparison between the p-S-N field predicted for fatigue crack initiation of riveted connections and experimental results for different stress ranges.

Finally, it is emphasized that this methodology also allows the hazard maps for the riveted joint to be determined making use of Eq. (4). The hazard maps, typically created for the analysis of natural disasters, are graphs that highlight the areas being affected or becoming vulnerable to a certain type of failure, providing visual information on the probability of occurrence of this phenomenon at each particular point of the studied space. Occasionally, they are also used to display the failure hazard of mechanical and structural components as a distribution of the generalized parameter for the critical acting load. Accordingly, the same concept can be extended to any structural fatigue design when the PFCDF is known, because the local probability of crack initiation may be estimated from the stress, strain or any other GP distribution, which represents conveniently the fatigue damage process. Thereby, in the example of application presented in this paper, each local value of the strain range is related to the probability of failure taking into account the size of the elements pertaining to the mesh designed. Figure 14 illustrates the strain range map and the hazard map for the central plate of the riveted joint, this being the critical one. Since only the fatigue crack initiation is envisaged, only surface values are represented in Fig. 14.

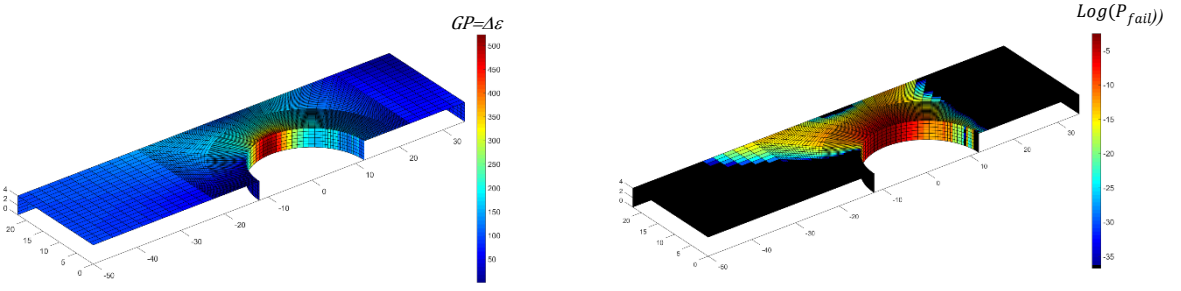

Figure 14. a) Strain range distribution (left) and b) the corresponding hazard maps (distribution of ($Log(P_{fail})$) for a riveted joint subjected to a $\Delta\sigma$= 170 MPa during 50,000 cycles.

In the design stage, but also along the lifetime of the component, the hazard maps complement the information provided by the global probability of failure. Thus, while the latter informs whether the component fulfills the safety requirements as a whole, the former permits the identification of the local critical points in the current design giving advice about the possible convenience of improving such weak points by proceeding to a local redesign of the component.

5. Conclusions

A methodology, based on the generalized local approach and the Weibull model proposed by Castillo-Canteli, is applied to derive the primary failure cumulative distribution function for prediction of fatigue crack initiation. The approach is applicable to any kind of test, irrespective of the specimen size and geometry or load type, allowing a suitable and reliable consideration of the statistical size effect.

The methodology represents an extension of the local methodology applied to quasi-static failure prediction of brittle materials. In addition, it takes into account the local value of a generalized parameter, suitably selected for fatigue crack initiation, as obtained from a finite element calculation, without requiring an analytical description of the distribution. It is worth mentioning that the methodology presented in this paper is applicable to any fatigue failure criterion.

In this way, higher generality is achieved by applying this model in comparison with other current solutions. This represents an important advance for fatigue life prediction because the influence of the distribution of this parameter rather than only the maximum value of the critical parameter is considered in the fatigue lifetime prediction.

An extension of the proposed methodology to the prediction of the total fatigue life of components, including the fatigue crack propagation phase, would require the consideration of the volume size effect by integration of a convenient fatigue crack propagation law.

Acknowledgements

The authors gratefully acknowledge the Severo Ochoa Pre-doctoral Grants Program of the Regional Government of Asturias (Spain) and the Spanish Ministry of Science and Innovation (MICINN) under project BIA2010-19920 for funding support. The authors also acknowledge the Portuguese Science Foundation (FCT) for the financial support through the post-doctoral grant SFRH/BPD/107825/2015. Finally, authors gratefully acknowledge the funding of SciTech - Science and Technology for Competitive and Sustainable Industries, R&D project co-financed by Programa Operacional Regional do Norte ("NORTE2020"), through Fundo Europeu de Desenvolvimento Regional (FEDER).

References

1. Carpinteri A., Spagnoli A., Vantadori S. (2002). An approach to size effect in fatigue of metals using fractal theories. Fatigue & Fracture of Engineering Materials and Structures - ISSN: 8756758X, Vol. 25, No. 7, 619-627, doi: 10.1046/j.1460-2695.2002.00506.x

2. Carpinteri A., Spagnoli A., Vantadori S. (2009). Size effect in S-N curves: A fractal approach to finite-life fatigue strength. International Journal of Fatigue - ISSN: 01421123, Vol. 31, No. 5, 927-933, doi: 10.1016/j.ijfatigue.2008.10.001

3. Spagnoli A., Vantadori S., Carpinteri A. (2015), Interpreting some experimental evidences of fatigue crack size effects through a kinked crack model. Fatigue and Fracture of Engineering Materials and Structures - ISSN: 8756758X, Vol. 38, 215-222, doi: 10.1111/ffe.12185

4. Bastenaire F.A. (1972). New method for the statistical evaluation of constant stress amplitude fatigue-test results, Tech. Rep., ASTM, Philadelphia Ph.

5. Bogdanoff J.L., Kozin F. (1985). Probabilistic models of cumulative damage, Wiley, New York.

6. Escobar L.A., Meeker W.Q. (1999). Statistical prediction based on censored life data, Technometrics, Vol. 41, No. 2, 113-124.

7. Pascual F.G., Meeker W.Q. (1999), Estimating fatigue curves with the random fatigue-limit model, Technometrics 41, 277-302.

8. Spindel JE, Haibach E. (1981). Some considerations in the statistical determination of the shape of s − n curves. Statistical Analiysis of Fatigue Data. American Society for Testing Materials. ASTM STP 744, 89–113.

9. Schijve J. (2005). Statistical distribution functions and fatigue of structures. International Journal of Fatigue; 27, 1031–1039.

10. Bolotin V.V. (1999). Mechanics of fatigue, CRC Boca Ratón Fl.

11. Bolotin V.V. (1981). Wahrscheinlichkeitsmethoden zur Berechnung von Konstruktionen, Verlag für Bauwesen, Berlin.

12. Castillo E., Fernández-Canteli A. (2009). A unified statistical methodology for modeling fatigue damage. Springer.

13. Correia J., Apetre N., Arcari A., De Jesus A., Muñiz-Calvente M., Calçada R., Berto F., Fernández-Canteli A. (2017). Generalized probabilistic model allowing for various fatigue damage variables. International Journal of Fatigue; 100, 187-194.

14. Fernández-Canteli A., Przybilla C., Correia J. A. F. O., de Jesus A. M. P., Castillo, E. (2012). Extending the applicability of probabilistic S-N models to the LCF region using energetic damage parameters, In Proc. XVI Int.Colloquium Mechanical Fatigue of Metals, Brno.

15. Castillo E., López Aenlle M., Ramos A., Fernández Canteli A., Esslinger V., Kieselbach R. (2006). Specimen length effect on parameter estimation in modelling fatigue strength by Weibull distribution, Int. J. of Fatigue, 28, 1047-1058.

16. Muñiz-Calvente M., Fernández-Canteli A., Shlyannikov V., Castillo E. (2015). Probabilistic Weibull methodology for fracture prediction of brittle and ductile materials. Applied Mechanics and Materials, Vol. 784, 443-451.

17. Carpinteri, A., Fernández-Canteli, A., Fortese, G., Muñiz-Calvente, M., Ronchei, C., Scorza, D., Vantadori, S. (2017). Probabilistic failure assessment of Fibreglass composites Composite Structures, 160, 1163-1170.

18. Muñiz-Calvente M. (2017). The generalized local model: A methodology for probabilistic assessment of fracture under different failure criteria, Doctoral Thesis, University of Oviedo.

19. Przybilla C., Fernández-Canteli A., Castillo E. (2011). Deriving the primary cumulative distribution function of fracture stress for brittle materials from 3- and 4-point bending tests, J. Eur. Ceram. Soc., vol. 31, no. 4, 451–460.

20. Papazafeiropoulos G., Muñiz-Calvente M., Martínez-Pañeda E. (2017). Abaqus2Matlab: a suitable tool for finite element post-processing. Advances in Engineering Software, vol 105. 9-16. DOI:10.1016/j.advengsoft.2017.01.006

21. Fitting a Univariate Distribution Using Cumulative Probabilities - MATLAB & Simulink Example - MathWorks.

22. de Jesus A. M. P., da Silva A. L. L., Figueiredo M. V., Correia J. A. F. O., A. S. Ribeiro, Fernandes A. A. (2011). Strain-life and crack propagation fatigue data from several Portuguese old metallic riveted bridges, Eng. Fail. Anal., vol. 18, no. 1, 148–163.

23. Correia J. A. F. O., De Jesus A. M. P., Fernandez-Canteli A., Calçada R. A. B. (2015). Fatigue Damage Assessment of a Riveted Connection Made of Puddle Iron from the Fão Bridge using the Modified Probabilistic Interpretation Technique, Procedia Eng., vol. 114, 760–767.

24. ASTM E647-95 (1995), Standard Test Method for Measurement of Fatigue Crack Growth Rates. Annual Book of Standards, Part 10. West Conshohocken, Pa, USA.

25. Sanches R. F., A. M. P. de Jesus, Correia J. A. F. O., da Silva A. L. L., Fernandes A. A. (2015). A probabilistic fatigue approach for riveted joints using Monte Carlo simulation, J. Constr. Steel Res., vol. 110, 149–162.

26. de Jesus A. M. P., da Silva A. L. L., Correia J. A. F. O. (2014). Fatigue of riveted and bolted joints made of puddle iron—A numerical approach, J. Constr. Steel Res., vol. 102, 164–177.

27. ANSYS. Swanson Analysis Systems Inc, Houston (2009).

28. Kalnins A. (2006), Fatigue Analysis in Pressure Vessel Design by Local Strain Approach: Methods and Software Requirements, J. Press. Vessel Technol., vol. 128, no. 1, 2.